Rangsit Journal of Arts and Sciences, July-December 2012 RJAS Vol. 2 No. 2, pp. 151-160

DOI : 10.14456/rjas.2012.15

Immersion and Invariance-Based nonlinear controller for a Power System with the excitation and STATCOM

Adirak Kanchanaharuthai

Department of Electrical Engineering, College of Engineering,
Rangsit University, Patumthani 12000 Thailand
E-mail: adirak@rsu.ac.th

Submitted 28 June 2012; accepted in final form 24 September 2012

Abstract

In this paper, based on Immersion and Invariance (I&I) methodology, a nonlinear excitation and Static Synchronous Compensator (STATCOM) controller is proposed for the transient stability enhancement of an electrical power system. In particular, the simplified nonlinear model of power system elements and I&I design method are used to achieve not only power angle stability but also frequency and voltage regulations during a large (disturbance) perturbation (a symmetrical three-phase short circuit fault) on the transmission lines. The simulation results show that the proposed controller can not only keep the system transiently stable under severe disturbances but also simultaneously achieve power angle stability as well as frequency and voltage regulation.

Keywords: *Transient stability, generator excitation, STATCOM, Immersion and Invariance methodology*.

บทคัดย่อ

บทความนี้นำเสนอตัวควบคุมการกระตุ้นของเครื่องกำเนิดไฟฟ้าซิงโครนัสและตัวชดเชยซิงโครนัสแบบสถิตที่ไม่เป็นเส้นด้วยวิธีการฝังในและความยืนยงเพื่อเพิ่มเสถียรภาพชั่วครู่ของระบบไฟฟ้ากำลัง เพื่อออกแบบตัวควบคุมแบบจำลองที่ไม่ซับซ้อนของระบบไฟฟ้าและวิธีการฝังในและความยืนยงถูกนำมาใช้เพื่อบรรลุเสถียรภาพของมุมกำลังและการควบคุมความถี่และแรงดันขณะที่มีสัญญาณรบกวนขนาดใหญ่บนสายส่งไฟฟ้า เช่นการเกิดกระแสลัดวงจรสามเฟสแบบสมมาตร จากผลการจำลองด้วยคอมพิวเตอร์ ตัวควบคุมนำเสนอสามารถทำให้ระบบมีเสถียรภาพแบบชั่วครู่ภายใต้สัญญาณรบกวนที่รุนแรง และยังบรรลุเสถียรภาพของมุมกำลังพร้อมทั้งการควบคุมความถี่และแรงดันของระบบไฟฟ้ากำลัง

คำสำคัญ: *Transient stability, generator excitation, STATCOM, Immersion and Invariance methodology.*

1. Introduction

Continuing developments in power electronic devices have resulted in the development of reliable and high speed Flexible AC Transmission System (FACTS) devices. FACTS are employed mainly to improve the controllability of power flow and voltages augmenting the utilization and stability and are common equipment in the power industry. In addition, they have been used to replace a significant number of mechanical control devices (Song & John, 1999; Hingorani & Gyugyi, 1999). Applications for FACTS are often employed in interconnected and long-distance transmission systems to improve several technical problems, e.g. load flow control, voltage control, system oscillations, inter-area oscillation, reactive power control, steady state stability, and dynamic stability.

As one of the most promising FACTS devices, the Static Synchronous Compensator (STATCOM) is of particular interest in this study since this device can increase the grid transfer capability through enhanced voltage stability, significantly provide not only smooth and rapid reactive power compensation for voltage support but also improve both damping oscillation and transient stability.

The objective of this paper is to investigate the transient stability enhancement via the incorporation of a generator excitation and STATCOM. It is well-known that the transient stability is associated with dynamic behavior of the trajectories before the fault is cleared from the system. Therefore, the question of interest becomes whether, when the fault is cleared from the network, will the system settle to a post-fault equilibrium state.

So far, the excitation and STATCOM have separately been used to improve power system operations. The use of a coordination of excitation and STATCOM to improve voltage stability and to regulate active power and improve frequency stability, provides an opportunity to improve overall small-signal and transient stability of the power system.

Unfortunately, relatively little prior research based on the nonlinear control theory has been devoted to the combination of excitation and STATCOM (Liu, Sun, Shen, & Song, 2003; Gu & Wang, 2007).

More recently, Kanchanaharuthai, Chankong, & Loparo (2011a, 2011b, 2012) have shown the combination of excitation and STATCOM for transient stability and voltage regulation enhancement via an Interconnection and Damping Assignment-Passivity Based Control (IDA-PBC) methodology for power systems with distributed renewable energy resources that include excitation, STATCOM, and battery energy storage.

This paper continues this line of investigation and concentrate on how an excitation and STATCOM system can be employed using I&I methodology to enhance the transient stability of power systems interconnected to the grid. Using I&I design, the coordinated (Excitation/ STATCOM) controller, proposed in this paper, can simultaneously achieve angle stability as well as frequency and voltage regulation. In particular, it can provide additional benefits beyond the excitation alone and a conventional PSS/AVR controller.

The paper is organized as follows. The problem formulation is provided in Section 2. Simplified dynamic models of SG and STATCOM are briefly described and an analysis of transmitted power including STATCOM is considered in Section 3. I & I controller design is given in Section 4. Simulation results are given in Section 5. Conclusions are given in Section 6.

2. Problem Statement

In this paper we are interested in studying the transient stability of a nonlinear power system including excitation and STATCOM. The nonlinear system considered can be written in the general form as follows:

$$\dot{x}(t) = f(x) + g(x)u(x) \tag{1}$$

where $x \in \mathbb{R}^n$ is the state variable, $u \in \mathbb{R}^m, m < n$ is the control action, and $g(x)$ is assumed full rank.

The problem of interest in this paper is the following: given a stable equilibrium point x_e find a controller law $u(x)$ so that the closed-loop system satisfies the following:

1. The system is asymptotically and transiently stable at a desired equilibrium point x_e.
2. Power angle stability along with voltage and frequency regulations is simultaneously achieved.

In the next section, we provide the simplified nonlinear models of power system elements and use these models to design a state feedback control law that meets these requirements.

3. Power System Model and Transmitted with STATCOM

In this section, the dynamic models of the power systems elements employed in this paper are briefly provided.

A. Synchronous Generator: SG

A dynamic model of a synchronous generator (SG) in a Single Machine Infinite Bus (SMIB) system can be obtained by representing the SG by a transient voltage source, E, behind a direct axis transient reactance, X_d' as follows:

$$\begin{aligned}
\dot{\delta} &= \omega - \omega_s \\
\dot{\omega} &= \frac{1}{M}\left(P_m - P_E - D(\omega - \omega_s)\right) \\
\dot{E} &= -\frac{X_{d\Sigma}}{X_{d\Sigma}'T_0'}E + \frac{\left(X_{d\Sigma}' - X_{d\Sigma}\right)}{X_{d\Sigma}'T_0'}V_\infty \cos\delta + \frac{u_f}{T_0'}
\end{aligned} \tag{2}$$

where δ is the power angle of the generator, ω denotes the relative speed of the generator, $D \geq 0$ is a damping constant, P_m is the mechanical input power, $P_E = EV_\infty \sin\delta / X_{d\Sigma}'$ is the electrical power, without STATCOM, delivered by the generator to the voltage at the infinite bus V_∞ is the synchronous machine speed, $\omega = 2\pi f$, H represents the per unit inertial constant, f is the system frequency and $M = 2H/\omega_s$. $X_{d\Sigma}' = X_d' + X_T + X_L$ is the reactance consisting of the direct axis transient reactance of SG, the reactance of the transformer, and the reactance of the transmission line. Similarly, $X_{d\Sigma} = X_d + X_T + X_L$ is identical to $X_{d\Sigma}'$ except that X_d denotes the direct axis reactance of SG. T_0' is the direct axis transient short-circuit time constant. u_f is the field voltage control input to be designed.

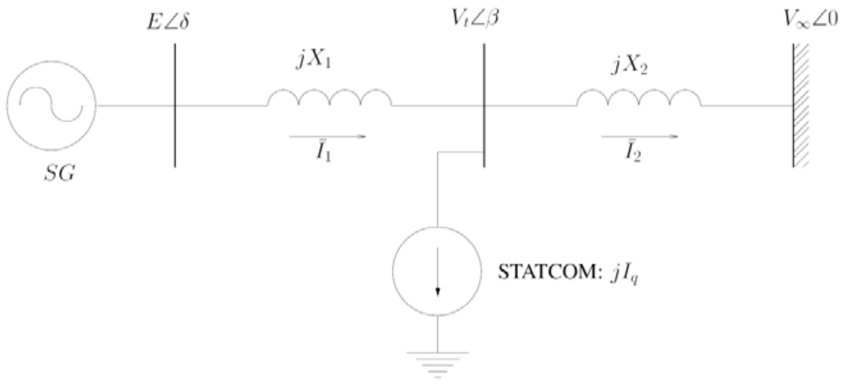

Figure 1 Network

B. STATCOM Model

STATCOM can be employed to support electrical power networks that have poor voltage and power stability (both small-signal and large-signal (transient)), (Song & John, 1999 ; Hingorani & Gyugyi, 1999) and references therein. For simplicity, the dynamic behavior of the STATCOM is regarded as a first-order differential equation; thus, the STATCOM dynamic model is expressed as follows:

$$\dot{I}_q = \frac{1}{T}(-(I_q - I_{qe}) + u_q) \tag{3}$$

where I_q denotes the injected or absorbed STATCOM currents as a controllable current source, I_{qe} is an equilibrium point of STATCOM currents, u_q is the STATCOM control input to be designed, and T is a time constant of STATCOM models.

C. Transmitted Power with STATCOM

In this subsection, we study the transmitted power characteristics of conventional power generators, especially SG, when STATCOM is included. We assume that any losses in the STATCOM are negligible, and we model the STATCOM system as a shunt current source. We focus on the transmitted power in the SMIB system as a shunt current source. We focus on the transmitted power in the SMIB.

Consider the network shown in Figure 1 where X_1 (or $X_d' + X_T$) denotes the reactance which takes into account the direct axis transient reactance X_d' of the SG and the transformer reactance X_T. X_2 (or X_L denotes the transmission line reactance between the bus terminal voltage V_t and the infinite bus voltage V_∞. I_q denotes the STATCOM current that is always quadrature with its bus terminal voltage. E is the transient voltage of the SG. Using some length but straightforward, calculation (Song & John, 1999; Kanchanaharuthai et al, 2011a) we have the power, P_E, transmitted from SG to the infinite bus is:

$$\begin{aligned} P_E &= P_e + P_s \\ &= \frac{EV_\infty \sin\delta}{(X_1+X_2)} + \frac{EV_\infty \sin\delta}{(X_1+X_2)}\frac{I_q X_1 X_2}{\Delta(\delta,E)} \end{aligned} \tag{4}$$

where

$$\Delta(\delta,E) = \sqrt{(EX_2)^2 + (V_\infty X_1)^2 + 2X_1X_2EV_\infty \cos\delta}$$

4. Immersion and Invariance

The I&I method has been first proposed in Astolfi & Oreta (2003), and Astolfi, Karagiannis, & Oreta (2007), and employed in its wide range of applications, such as observed design, stabilization, and adaptive control for nonlinear systems. The theories, discovered in those papers, have been used to design this proposed nonlinear coordinated controller for power systems including STATCOM.

Theorem 1: Consider the nonlinear system[1] (Astolfi & Oreta, 2003; Astolfi et al., 2007)

$$\dot{x}(t) = f(x) + g(x)u(x) \tag{5}$$

[1] It is assumed that all functions and mappings are $\mathbb{C}^\infty$ throughout this paper

with state $x \in \mathbb{R}^n$ and control input $u \in \mathbb{R}^m$, and an assignable equilibrium point $x_e \in \mathbb{R}^n$ to be stabilized. Let $s < n$, and assume that there exist smooth mappings

$$\alpha : \mathbb{R}^s \to \mathbb{R}^s, \pi : \mathbb{R}^s \to \mathbb{R}^n, c : \mathbb{R}^n \to \mathbb{R}^m,$$
$$\phi : \mathbb{R}^n \to \mathbb{R}^{n-s}, \varphi : \mathbb{R}^{n\times(n-s)} \to \mathbb{R}^m,$$

such that the following hold.

(H1) (Target system) The system

$$\dot{\xi} = \alpha(\xi) \tag{6}$$

with state $\xi \in \mathbb{R}^s$, has an asymptotically stable equilibrium at $\xi_e \in \mathbb{R}^s$ and $x_e = \pi(\xi_e)$

(H2) (Immersion condition) For all $\xi \in \mathbb{R}^s$

$$f(\pi(\xi)) + g(\pi(\xi))c(\pi(\xi)) = \frac{\partial \pi(\xi)}{\partial \xi}\alpha(\xi) \tag{7}$$

(H3) (Implicit manifold) The following set identity holds.

$$\mathcal{M} := \{x \in \mathbb{R}^n \mid x = \pi(\xi) \text{ for some } \xi \in \mathbb{R}^s\}$$
$$= \{x \in \mathbb{R}^n \mid \phi(x) = 0\} \tag{8}$$

(H4) (Manifold attractivity and trajectory boundedness)

All trajectories of the system

$$\begin{aligned} \dot{z} &= \frac{\partial \phi(x)}{\partial x}[f(x) + g(x)\varphi(x,z)], \\ \dot{x} &= f(x) + g(x)\varphi(x,z) \end{aligned} \tag{9}$$

are bounded and satisfy $\lim_{t\to+\infty} z(t) = 0$.

Then, x_e is a globally asymptotically stable equilibrium of the closed loop system

$$\dot{x} = f(x) + g(x)\varphi(x, \phi(x)) \tag{10}$$

As looking back to the dynamic equations of power system including SG and STATCOM in (2)-(4) and defining the state variables $x_1 = \delta$, $x_2 = \omega - \omega_s, x_3 = E, x_4 = I_q$ those dynamic models can be expressed as the general forms in (1) or (5), i.e.,

$$f(x) = \begin{bmatrix} x_2 \\ \frac{1}{M}\left(P_m - \frac{x_3 V_\infty \sin x_1}{X_1 + X_2}\left(1 + \frac{x_4 X_1 X_2}{\Delta(x_1, x_3)}\right)\right) \\ -a x_3 + b\cos x_1 \\ -\frac{1}{T}(x_4 - x_{4e}) \end{bmatrix},$$

$$g(x) = \begin{bmatrix} 0 & 0 \\ 0 & 0 \\ 1 & 0 \\ 0 & 1 \end{bmatrix},\ u(x) = \begin{bmatrix} \frac{u_f}{T_0'} \\ \frac{u_q}{T} \end{bmatrix} \tag{11}$$

where $a = \frac{X_s}{(X_1 + X_2)T_0'}$ and $b = \frac{X_m V_\infty}{(X_1 + X_2)T_0'}$.

The open loop operating equilibrium is denoted by $x_e = [x_{1e}, 0, E, 0]^T$ and the region of operation is defined in the set as follows:

$$\mathcal{D} = \{x \in \mathcal{S} \times \mathbb{R} \times \mathbb{R} \times \mathbb{R} \mid 0 < x_1 < \frac{\pi}{2}\}.$$

4.1 I&I Controller Design

4.1.1 Target system

In order to design a stabilizing controller and verify the condition according to Theorem 1, we start with selecting the target dynamics as the mechanical subsystems (e.g., a simple damped pendulum system)

$$\begin{aligned} \dot{\xi}_1 &= \xi_2, \\ \dot{\xi}_2 &= -\frac{\partial V(\xi_1)}{\partial \xi_1} - R(\xi)\xi_2 \end{aligned} \tag{12}$$

where $V(\xi_1)$ and $R(\xi)$ represent the potential energy and damping function of the pendulum systems, respectively, both of which are to selected. The pendulum system, considered with a stable equilibrium point $\xi_e = (\xi_{1e}, 0)^T$, has the potential energy $V(\xi_1)$ satisfying the following two assumptions: (i) $\frac{\partial V(\xi_{1e})}{\partial \xi} = 0$ (ii) $\frac{\partial^2 V(\xi_{1e})}{\partial^2 \xi} > 0$ and the damping function verifying $R(\xi_e) \geq 0$. It is easy to choose the potential energy $V(\xi_1)$ along conditions as $V(\xi_1) = -\beta \cos\tilde{\xi}_1, \tilde{\xi}_1 = \xi_1 - \xi_{1e}, \ \exists \beta > 0$.

4.1.2 Immersion condition

As the desired target system has been already selected, a mapping $\pi : \mathcal{S} \times \mathbb{R} \to \mathcal{S} \times \mathbb{R} \times \mathbb{R} \times \mathbb{R}$ is determined as follows.

$$\pi(\xi_1, \xi_2) := (\xi_1,\ \xi_2,\ \pi_3(\xi),\ \pi_4(\xi))^T, \tag{13}$$

where both $\pi_3(\xi)$ and $\pi_4(\xi)$ are selected. Besides, the condition of Theorem 1 gives the constraints, namely $\xi_{1e} = x_{1e}, \xi_{2e} = x_{2e}, \xi_{3e} = x_{3e}, \xi_{4e} = x_{4e}$. We can choose $\pi_3(\xi)$ and $\pi_4(\xi)$ to satisfy the condition (7), especially the second row as shown below.

$$\begin{bmatrix} \xi_2 \\ \frac{1}{M}\left[P_m - \frac{\pi_3(\xi)V_\infty \sin\xi_1}{(X_1+X_2)} \cdot \left(1 + \frac{\pi_4(\xi)X_1X_2}{\Delta(\xi_1,\pi_3(\xi))}\right)\right] - \frac{D}{M}\xi_2 \\ -a\pi_3(\xi) + b\cos\xi_1 \\ -\frac{1}{T}(\pi_4(\xi) - x_{4e}) \end{bmatrix}$$

$$+\begin{bmatrix} 0 & 0 \\ 0 & 0 \\ 1 & 0 \\ 0 & 1 \end{bmatrix}\begin{bmatrix} c_1(\pi(\xi)) \\ c_2(\pi(\xi)) \end{bmatrix} = \begin{bmatrix} 1 & 0 \\ 0 & 1 \\ \frac{\partial \pi_3}{\partial \xi_1} & \frac{\partial \pi_3}{\partial \xi_2} \\ \frac{\partial \pi_4}{\partial \xi_1} & \frac{\partial \pi_4}{\partial \xi_2} \end{bmatrix}\begin{bmatrix} \xi_2 \\ -\frac{\partial V(\xi_1)}{\partial \xi_1} - R(\xi)\xi_2 \end{bmatrix}$$

$$= \begin{bmatrix} 1 & 0 \\ 0 & 1 \\ \frac{\partial \pi_3}{\partial \xi_1} & \frac{\partial \pi_3}{\partial \xi_2} \\ \frac{\partial \pi_4}{\partial \xi_1} & \frac{\partial \pi_4}{\partial \xi_2} \end{bmatrix}\begin{bmatrix} \xi_2 \\ -\beta\sin\tilde{\xi}_1 - \frac{\gamma_d + D}{M}\xi_2 \end{bmatrix}, \gamma_d \geq 0$$

From the expression above, in order to simplify our derivations, $\pi_3(\xi)$ is chosen as a constant, that is, $\pi_3(\xi) = x_{3e}$. Consequently, we can compute $\pi_4(\xi)$ as follows:

$$\pi_4(\xi) = \left(P_m + \beta M \sin\tilde{\xi}_1 + \gamma_d \xi_2 - \frac{\pi_3 V_\infty \sin\xi_1}{X_1 + X_2}\right) \cdot \frac{X_1 + X_2}{\pi_3 V_\infty \sin\xi_1} \cdot \frac{\Delta(\xi_1, \pi_3)}{X_1 X_2} \quad (14)$$

As the mapping $\pi(\xi)$ has been chosen, by using some lengthy, but straightforward, calculation from the third and forth rows, respectively, we have the control input below that renders the manifold $\mathcal{M}$ invariant.

$$\left(\frac{u_f}{T_0^{'}}, \frac{u_q}{T}\right)^T = \left(c_1(\pi(\xi)), c_2(\pi(\xi))\right)^T$$

4.1.3 Implicit Manifold

From the results above, the mapping $\pi(\xi)$ has been defined and the condition in (8) is verified. It is obvious that the mapping $\phi(x)$ can be defined as follows:

$$\phi(x) = \begin{pmatrix} x_3 - \pi_3(x_1, x_2) \\ x_4 - \pi_4(x_1, x_2) \end{pmatrix} \quad (15)$$

4.1.4 Manifold attractivity and trajectory boundedness:

In this subsection, a control law $u = \varphi(x, z)$ is designed to ensure that all trajectories of the closed-loop system are bounded and converge to the manifold $\mathcal{M}$. Let $z := \phi(x)$ be the off-the-line manifold coordinate, substituting $\dot{x}_3$ and $\dot{x}_4$ into the expression below we have

$$\dot{z}_1 = \dot{x}_3 = -ax_3 + b\cos x_1 + \frac{\varphi_1(x,z)}{T_0^{'}},$$

$$\begin{aligned} \dot{z}_2 &= \dot{x}_4 - \dot{\pi}_4(x_1, x_2) \\ &= \frac{-(x_4 - x_{4e}) + \varphi_2(x,z)}{T} - \frac{\partial \pi_4}{\partial x_1}\dot{x}_1 - \frac{\partial \pi_4}{\partial x_2}\dot{x}_2 \end{aligned},$$

In order to ensure that the trajectories of the off-the-manifold coordinate z are bounded and $\lim_{t\to+\infty} z(t) = 0$ according to condition (10), we take $\dot{z}_i = -\gamma_i z_i, \gamma_i > 0, i = 1,2$ and then we get

$$\frac{\varphi_1(x,z)}{T_0^{'}} = ax_3 - b\cos(x_1) - \gamma_1 z_1,$$

$$\frac{\varphi_2(x,z)}{T} = \frac{(x_4 - x_{4e})}{T} + \frac{\partial \pi_4}{\partial x_1}\dot{x}_1 + \frac{\partial \pi_4}{\partial x_2}\dot{x}_2 - \gamma_2 z_2$$

4.1.5 The control law: We can compute the control laws as follows:

$$\begin{aligned} \frac{u_f}{T_0^{'}} &= \frac{\varphi_1(x,\phi(x))}{T_0^{'}} \\ &= ax_3 - b\cos(x_1) - \gamma_1(x_3 - x_{3e}), \\ \frac{u_q}{T} &= \frac{\varphi_2(x,\phi(x))}{T} \\ &= \frac{(x_4 - x_{4e})}{T} + \frac{\partial \pi_4}{\partial x_1}\dot{x}_1 + \frac{\partial \pi_4}{\partial x_2}\dot{x}_2 - \gamma_2(x_4 - \pi_4(x_1, x_2)) \end{aligned} \quad (16)$$

where $\frac{\partial \pi_4}{\partial x_1}$ and $\frac{\partial \pi_4}{\partial x_2}$ are straightforwardly computed and provided below, while $\dot{x}_1$ and $\dot{x}_2$ are determined from (11).

$$\begin{aligned} \frac{\partial \pi_4}{\partial x_1} &= \frac{(X_1 + X_2)\Delta(x_1, x_{3e})\mathcal{L}}{V_\infty X_1 X_2 x_{3e} \sin x_1} \\ &\quad - x_{3e}(X_1 + X_2)\mathcal{P} - \frac{\cos x_1 (X_1 + X_2)\Delta(x_1, x_{3e})\mathcal{P}}{V_\infty X_1 X_2 x_{3e} \sin^2 x_1}, \\ \frac{\partial \pi_4}{\partial x_2} &= \gamma_d \frac{(X_1 + X_2)\Delta(x_1, x_{3e})}{x_{3e} V_\infty X_1 X_2 \sin x_1}, \end{aligned}$$

$$\mathcal{L} = M\beta\cos(x_1 - x_{1e}) + \frac{V_\infty x_{3e}\cos x_1}{X_1 + X_2},$$
$$\mathcal{P} = P_m + \gamma_d x_2 + M\beta\sin(x_1 - x_{1e}) + \frac{V_\infty x_{3e}\sin x_1}{X_1 + X_2} \tag{17}$$

According to the condition (H4), it is also necessary to prove boundedness of the trajectories of the closed-loop system with the control law $\varphi_i(x,\phi(x)), i = 1,2$ and the off-the-manifold coordinate z as given below:

$$\begin{aligned}
\dot{x}_1 &= x_2,\\
\dot{x}_2 &= \frac{1}{M}\left(P_m - \frac{x_3 V_\infty \sin x_1}{X_1 + X_2}\left(1 + \frac{x_4 X_1 X_2}{\Delta(x_1, x_3)}\right)\right),\\
\dot{x}_3 &= -a x_3 + b\cos x_1 + \frac{u_f}{T_0'},\\
\dot{x}_4 &= -\frac{1}{T}(x_4 - x_{4e}) + \frac{u_q}{T},\\
\dot{z}_1 &= -\gamma_1 z_1, \qquad \dot{z}_2 = -\gamma_2 z_2.
\end{aligned} \tag{18}$$

We begin with the fact that clearly $x_1 \in \mathcal{S}$ is bounded and z_1 and z_2 are exponentially decaying functions, that is, $z_i(t) = z_i(0)e^{-\gamma_i t}, i = 1,2$ and also bounded. It follows that $x_3 = z_3 + \pi_3(\xi) = z_3 + x_{3e}$ is bounded. Also, there exists $\epsilon > 0$ such that, for all $x \in \mathcal{D}$, we have $|\Delta(x_1, x_3)| \geq \epsilon$. Substituting $x_3 = z_1 + x_{3e}$ and $x_4 = z_2 + \pi_4(x_1, x_2)$ into the second equation of (18) as well as using the energy function

$W = x_2^2/2 + V(x_1) + (z_1^2 + z_2^2)/2$, we have that

$$\begin{aligned}
\dot{W} &= -\frac{D+\gamma_d}{M}x_2^2 - \frac{k}{M}\frac{x_2 z_2 (z_1 + x_{3e})\sin x_1}{\Delta(x_1, x_3)} - \gamma_1 z_1^2 - \gamma_2 z_2^2,\\
&\leq -\frac{D+\gamma_d}{M}x_2^2 - \frac{k|x_2||z_1 z_2|}{M\epsilon} - \frac{k x_{3e}|x_2||z_2|}{M\epsilon}\\
&\quad -\gamma_1 z_1^2 - \gamma_2 z_2^2,\\
&\leq -\frac{D+\gamma_d + k x_{3e}\epsilon^{-1}}{M}x_2^2 - \left(\gamma_1 + \frac{k}{2M\epsilon x_{3e}^4}\right)z_1^2\\
&\quad -\left(\gamma_2 + \frac{k x_{3e}}{2M\epsilon}\right)z_2^2 \leq 0
\end{aligned}$$

where $k = X_1 X_2 / (X_1 + X_2)$ and the first inequality follows from Young's inequality, i. e. $2ab \leq ca^2 + b^2/c$ to eventually obtain the final inequality. From the last inequality above, $\gamma_1, \gamma_2, x_{3e}, k$ are positive and $D \geq 0, \gamma_d \geq 0$; thus resulting in boundedness of (x_1, x_2). This also implies boundedness of $\pi_4(x_1, x_2)$. Finally, boundedness of x_3 and x_4 follows from the fact that $x_3 = z_1 + x_{3e}$ and $x_4 = z_2 + \pi_4(x_1, x_2)$.

Hence, boundedness of the trajectories of (18) and $\lim_{t\to\infty} z(t) = 0$ have been shown. We can establish the main result summarizing the proposed I&I controller design in the following proposition.

Proposition 1: The closed-loop system (18) with the control laws (16) is locally asymptotically stable in x_e

Proof: The proof of proposition 1 is based on the arguments as given above in (12)-(15).

5. Simulation Results

In this section, simulation results of coordination of generator excitation and STATCOM in SMIB model considered in previous sections are shown using power angle stability as well as voltage and frequency regulations to point out the transient stability enhancement and dynamic properties.

Consider the single line diagram as shown in Figure 2 with SG connected through parallel transmission line to an infinite-bus. Such generators deliver 1.0 per unit, power while the terminal voltage V_t is 0.9897 pu., and an infinite-bus voltage is 1.0 per unit. However, when there is a three-phase fault (a large perturbation) occurring at the point P, the midpoint of one of the transmission lines, this leads to rotor acceleration, voltage sag, and large transient induced electromechanical oscillations.

We are, therefore, interested in the following question. After the fault is cleared from the network, will the system settle to a post-fault equilibrium state?

In this paper, the fault of interest is the following two fault sequences, namely temporary and permanent faults. Usually, there are four basic stages as sociated with transient stability studies (temporary and permanent faults) of a power system:

Stage 1: The system is in a pre-fault steady state.
Stage 2: A fault occurs at t_0.
Stage 3: The faults is isolated by opening the breakers at t_c.
Stage 4: The transmission line is recovered without the fault at $t = t_r$ sec. Eventually, the system is in a post-fault state at $t = t_f$ sec.

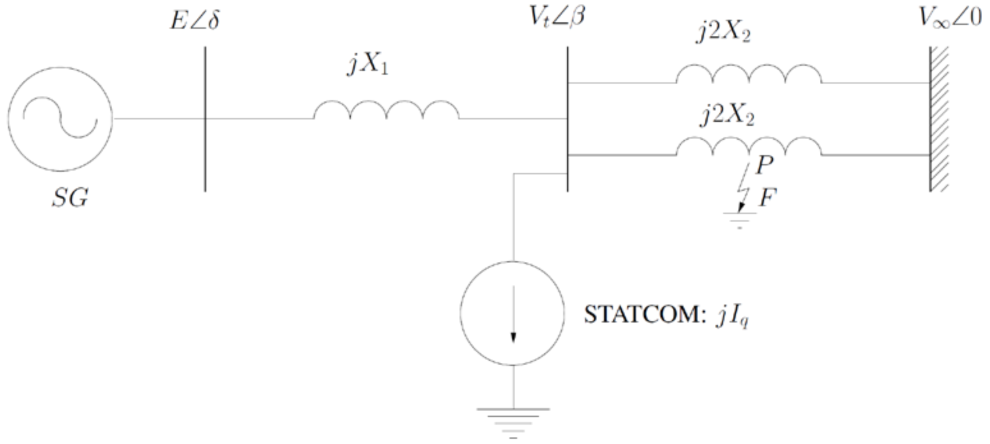

Figure 2 A single line diagram of SMIB

Temporary fault

The system is in a pre-fault steady state, a fault occurs at $t_0 = 0.5$ sec., the fault is isolated by opening the breaker of the faulted line at $t_c = 1$ sec., the transmission line is recovered without the fault at $t_r = 2$ sec. Afterward the system is in a post-fault state.

Permanent fault

The system is in a pre-fault steady state, a fault occurs at $t_0 = 0.5$ sec., the fault is isolated by permanently opening the breaker of the faulted line at $t_c = 1$ sec. The system is eventually in a post-fault state.

In this section, the effectiveness of the combination of the coordinated (Excitation /STAT-COM) controller to improve transient stability applied of a power system through power angle stability, as well as voltage, frequency, and power regulations, is investigated and compared with the excitation controller alone u_f (Dib, Kenne, & Lamnabhi-Lagarrigue, 2009) and a conventional PSS/AVR controller (Kundur, 1994) (The PSS/AVR parameters are specified, i.e.,

$K_{PSS} = 50, K_A = 4.5, T_e = 100, T_1 = 0.1$ and $T_2 = 0.025$

$$\omega_s = 2\pi f \text{ rad/s}, D = 0.2, M = 5, f = 60\,\text{Hz},$$
$$T_0^{'} = 4, V_\infty = 1\angle 0^\circ, X_d = 1.1, X_d^{'} = 0.2,$$
$$X_T = 0.1,\ X_2 = X_L = 0.2,\ T = 1,$$
$$P_m = 1, |I_q| \le 2, \delta_e = 0.4964\,\text{rad}, \omega = \omega_s,$$
$$E_e = 1.05, I_{qe} = 0, P_{se} = 0, P_{Ee} = P_{ee} = P_m,$$
$$V_t = V_{\text{ref}} = 0.9897, P_{Ee} = P_{ee} + P_{se} = P_m.$$

The physical parameters (pu.) and initial conditions ($\delta_e, \omega_s, E_e, I_{qe}$) for this proposed power system model are given as follows:

The tuning parameters of the coordinated controller selected to test in this paper are as follows: $\gamma_1 = \gamma_2 = \beta = 100$, and $\gamma_d = 1$. From our simulation results, the following can be seen.

The transient stability of a power system with both generator excitation and STATCOM can be effectively enhanced by using the nonlinear coordinated controller proposed as shown in Figures 3 and 4. Although there is a large sudden fault (temporary or permanent) on the network, the system is able to keep transiently stable.

Time histories of a power angle δ, SG relative speed (frequency) $\omega - \omega_s$, transient voltage E of the coordinated controller, excitation controller alone and PSS/AVR, respectively, are shown in Figures 3(a) and 4(a). After the fault is cleared from the network, from two fault cases above the power angles δ return to the pre-fault value δ_e and the SG relative speeds, $\omega - \omega_s \to 0$, settle to the pre-fault steady state as expected. Note also that, due to the presence of the permanent fault on the network, transient voltages E of the coordinated controller and PSS/AVR can go to the pre-fault state except for those of the excitation controller alone. In comparison with excitation alone and conventional controllers, time histories of the coordinated (excitation/STATCOM) controller, particularly power angles and relative speeds, have obviously smaller overshoot along with faster reduction of oscillation. Regarding power and voltage regulation as shown in Figure 3(b) and 4(b), the coordinated controller provides clearly better transient responses over excitation controller alone and PSS/AVR and quickly settles to their pre-fault steady state of active power. In particular, the voltage sag of the excitation/ STATCOM controller is quickly stabilized in comparison with excitation alone and PSS/AVR in terms of settling time and rise time but there are only higher overshoots. Their voltage responses also return to the desired reference voltage $V_{\text{ref}} = 0.9897$ pu., except for the permanent fault case, there is a change on network structure X_2. Figure 3(c) illustrates time histories of STATCOM current settling to the pre-fault steady state $\left(I_q \to 0\right)$ along with the off-the-manifold coordinates z_1 and z_2, showing the manifold $\mathcal{M}$ implicitly described by $\phi(x) = 0$. Figure 3(d) shows that after the fault is isolated, I_q and P_s from STATCOM becomes zero $(P_s \to 0)$. This causes $P_E \to P_{ee} = P_m$ to settle to the pre-fault state of active power of generator excitation and indicates that the combination of excitation and STATCOM can obviously improve further transient stability along with dynamic properties as compared with excitation alone and PSS/AVR. In other words, in the permanent fault, Figures 4(c)-(d) illustrate both I_s and P_s cannot return to the pre-fault state $\left(I_{qe} = 0, P_{se} = 0\right)$, because both are used to keep their power angles ($\delta \to \delta_e$), transient voltages $\left(E \to E_e\right)$, and active powers $\left(P_e + P_s \to P_{Ee}\right)$ constant excluding terminal voltages ($V_t \nrightarrow V_{\text{ref}}$).

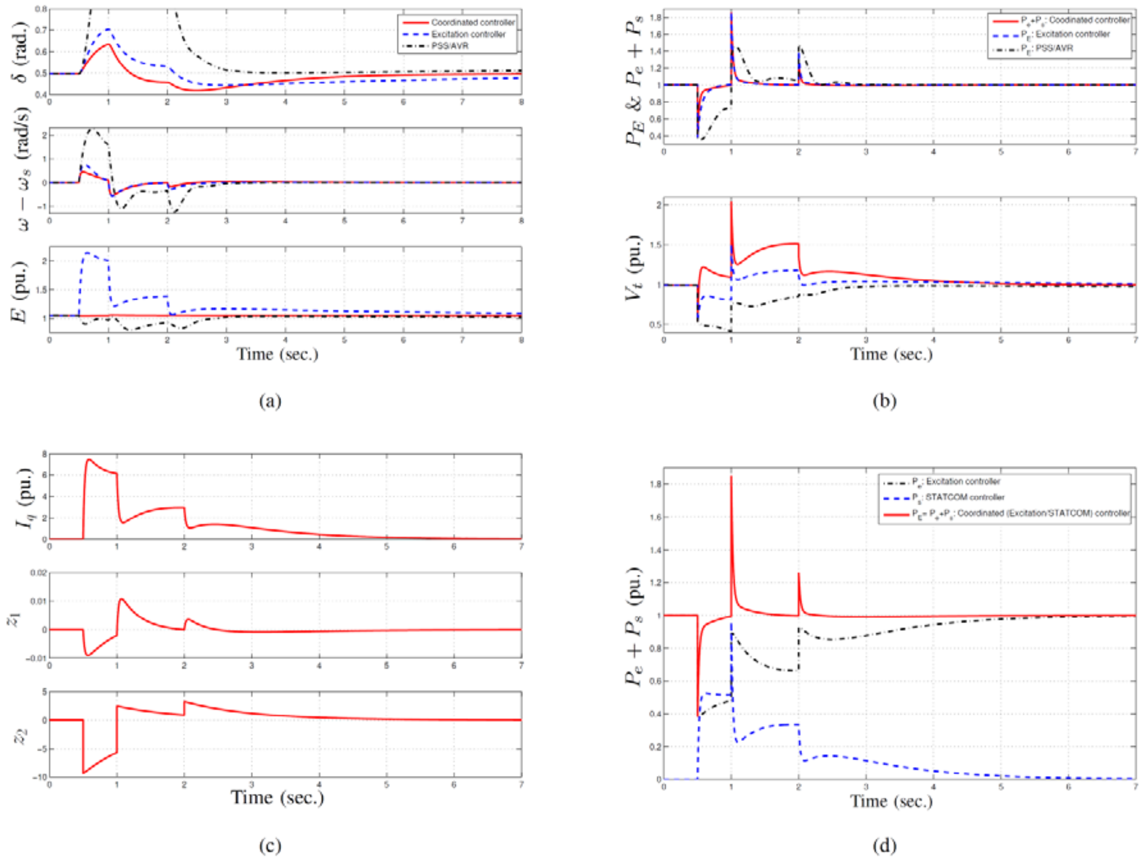

Figure 3 Temporary fault case: Time histories of (a) Power angle (δ), relative speed ($\omega - \omega_s$) and transient voltage (E), (b) Active power (P_E & $P_e + P_s$) and terminal voltage (V_t), (c) STATCOM current (I_q), and the off-the-line manifold coordinates z_1 and z_2, (d) Active power of coordinated (Excitation/STATCOM) controller (Solid: Coordinated controller, Dash: Excitation controller alone, Dashdot: PSS/AVR)

Also, the off-the-manifold coordinates z_1 and z_2 converge to zero, as expected. Independent of the steady-state operating point of the system and fault sequences above, the nonlinear coordinated controller can achieve the expected requirements and accomplish better dynamic properties as seen in faster transient responses (dynamic properties) of the closed-loop systems under a large sudden fault.

From the simulation results above, it can be concluded that not only transient stability is enhanced but also power angle stability as well as frequency, power, and voltage regulations are simultaneously achieved according to the expected requirements for the proposed controller.

6. Conclusions

In this paper, a nonlinear excitation and STATCOM controller, used to enhance the transient stability of a power system, has been proposed using I&I methodology. Simulation results have demonstrated that power angle stability along with voltage and frequency regulations are fulfilled the large (transient) disturbances on the network via I&I nonlinear model-based control design methodology. In particular, in spite of the occurrence of severe disturbances on the transmission line, the proposed coordinated controller proposed can not only maintain the transient stability but also accomplish better dynamic properties of the system while comparing to the operations with excitation alone and a conventional controller PSS/AVR.

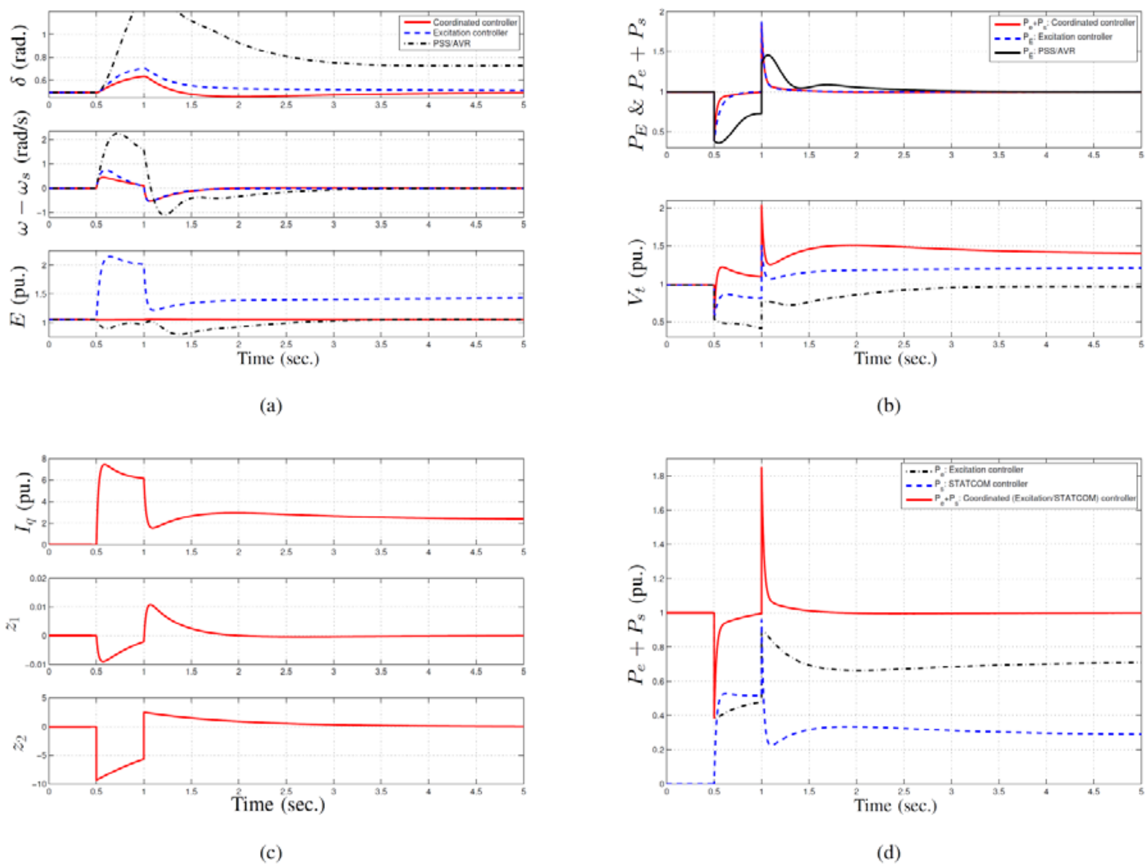

Figure 4 Permanent fault case: Time histories of (a) Power angle (δ), relative speed ($\omega - \omega_s$) and transient voltage (E), (b) Active power (P_E & $P_e + P_s$) and terminal voltage (V_t), (c) STATCOM current (I_q), and the off-the-line manifold coordinates z_1 and z_2, (d) Active power of coordinated (Excitation/ STATCOM) controller (Solid: Coordinated controller, Dash: Excitation controller alone, Dashdot: PSS/AVR)

7. References

Astolfi, A. & Oreta, R. (2003). Immersion and invariance: a new tool for stabilization and adaptive control of nonlinear systems. Trans. on Automatic Control, *48*, 590-606.

Astolfi, A., Karagiannis, D., & Oreta, R. (2007). Nonlinear and Adaptive Control Design and Applications. London, UK: Springer-Verlag.

Dib, W., Kenne, G., & Lamnabhi-Lagarrigue, F. (2009). An application of immersion and invariance to transient stability and voltage regulation of power systems with unknown mechanical power. Proc. Joint 48th IEEE CDC and 28th CCC, Shanghai, P.R. China.

Gu, L. & Wang, J. (2007). Nonlinear coordinated control design of excitation and STATCOM of power systems. Electric Power Systems Research, *77*, 788-796.

Hingorani, N.G. & Gyugyi L. (1999). Understanding FACTS: Concepts and Technology of Flexible AC Transmission Systems.

Kanchanaharuthai, A., Chankong, V., & Loparo, K. A. (2011a). Small-signal stability enhancement of power systems with renewable distributed energy resources. Proc. 18th IFAC World Congress, Milano, Italy.

Kanchanaharuthai, A., Chankong, V., & Loparo, K. A. (2011b). Transient stability and voltage regulation enhancement of power system with renewable distributed energy resources. Proc. IEEE 2011 EnergyTech Conference, OH, USA.

Kanchanaharuthai, A. (2012). Small-signal stability, transient stability, and voltage regulation enhancement of power systems with distributed renewable energy resources. Ph.D. Dissertation. Case Western Reserve University.

Kundur, P. (1994). Power System Stability and Control. Mc-Graw Hill.

Liu, Q. J., Sun, Y. Z., Shen, T. L., Song, & Y. H. (2003). Adaptive nonlinear coordinated excitation and STATCOM based on Hamiltonian structure for multimachine-power-system stability enhance ment. IEE Proceedings Contr. Theory and Appl., *150*, 285-294.

Song, Y. H. & John A. T. (1999). Flexible AC Transmission Systems (FACTS). London, UK: IEE Power and Energy Series 30.